Thermodynamics of PMMA/SAN Blends: Application of the Sanchez−Lacombe Lattice Fluid Theory

Gangyao Wen,[†] Zhaoyan Sun,[‡] Tongfei Shi,[†] Jian Yang,[†] Wei Jiang,[†] Lijia An,*[,†] and Binyao Li[†]

State Key Laboratory of Polymer Physics and Chemistry, Changchun Institute of Applied Chemistry, Chinese Academy of Sciences, Changchun 130022, P. R. China; and Research Center of Special Engineering Plastics, Department of Chemistry, Jilin University, Changchun 130023, P. R. China

Received January 8, 2001

ABSTRACT: Polymer blends of poly(methyl methacrylate) (PMMA) and poly(styrene-*co*-acrylonitrile) (SAN) with an acrylonitrile content of about 30 wt % were prepared by means of solution-casting and characterized by virtue of pressure−volume−temperature (*PVT*) dilatometry. The Sanchez−Lacombe (SL) lattice fluid theory was used to calculate the spinodals, the binodals, the Flory−Huggins (FH) interaction parameter, the enthalpy of the mixing, the volume change of the mixing, and the combinatorial and vacancy entropies of the mixing for the PMMA/SAN system. A new volume-combining rule was used to evaluate the close-packed volume per mer, v^*, of the PMMA/SAN blends. The calculated results showed that the new and the original volume-combining rules had a slight influence on the FH interaction parameter, the enthalpy of the mixing, and the combinatorial entropy of the mixing. Moreover, the spinodals and the binodals calculated with the SL theory by means of the new volume-combining rule could coincide with the measured data for the PMMA/SAN system with a lower critical solution temperature, whereas those obtained by means of the original one could not.

Introduction

Quite a few polymer solutions and mixtures exhibit lower critical solution temperature (LCST) phenomena,[1−7] which has fascinated scientists for many years. Early in 1942, Flory[8] and Huggins[9] gave the first description of the statistical thermodynamics of the phase equilibrium of polymer solutions and mixtures. The classical polymer solution theory, i.e., the Flory−Huggins (FH) theory,[10] which ignores the equation of state properties of the pure components, fails to describe the LCST behavior unless the interaction energy is known as a function of temperature and composition. To explain the LCST behavior, Flory, Orwoll, and Vrij (FOV)[11] developed a theory that incorporated the equation of state properties of the pure components. In the 1970s, Sanchez and Lacombe (SL) established the lattice fluid theory of pure fluids,[12] their solutions,[13] and their mixtures[14] which made allowances for empty lattice sites or free volume.

It has been known that poly(methyl methacrylate) (PMMA) and poly(styrene-*co*-acrylonitrile) (SAN) form a miscible blend when the acrylonitrile content in SAN is between about 9 and 33 wt %.[15,16] The miscible system exhibits an LCST phenomenon and has aroused great interest in scientists for both experiment and theory.[15−34] The miscibility of PMMA and SAN in the blend has been investigated by means of various methods such as infrared spectroscopy,[17,18] nuclear magnetic resonance,[19,20] electron microscopy,[21,22] laser light scattering,[16,23,24] neutron scattering,[25,26] differential scanning calorimetry,[15,16,27−29] shear measurement,[30,31] and pressure−volume−temperature (*PVT*) dilatometry.[32,33]

In this work, PMMA, SAN, and their blends were characterized with the aid of *PVT* dilatometry, and the resulting *PVT* data in the melt state were fitted to the SL equations of state. The spinodals, the binodals, the FH interaction parameter, the enthalpy of the mixing, the volume change of the mixing, and the combinatorial and vacancy entropies of the mixing for the PMMA/SAN system were calculated on the basis of the SL lattice fluid theory. Temperature and blend composition dependences of the calculated results are discussed in detail.

Theoretical Background

According to the SL lattice fluid theory,[12−14] the equations of state and the Gibbs energy per mer, $\bar{G}$, can be respectively expressed, for component i ($i = 1, 2$), as

$$\tilde{\rho}_i^{\,2} + \tilde{P}_i + \tilde{T}_i[\ln(1 - \tilde{\rho}_i) + (1 - 1/r_i^0)\tilde{\rho}_i] = 0 \qquad (1)$$

$$\bar{G}_i = \frac{G_i}{r_i^0 N_i} = \epsilon^*_{ii}\left\{-\tilde{\rho}_i + \tilde{P}_i\tilde{v}_i + \tilde{T}_i\left[(\tilde{v}_i - 1)\ln(1 - \tilde{\rho}_i) + \frac{1}{r_i^0}\ln\left(\frac{\tilde{\rho}_i}{\omega_i^0}\right)\right]\right\} \qquad (2)$$

and for the binary mixture as

$$\tilde{\rho}^2 + \tilde{P} + \tilde{T}[\ln(1 - \tilde{\rho}) + (1 - 1/r)\tilde{\rho}] = 0 \qquad (3)$$

$$\bar{G}_M = \frac{G_M}{rN} = \epsilon^*\left\{-\tilde{\rho} + \tilde{P}\tilde{v} + \tilde{T}\left[(\tilde{v} - 1)\ln(1 - \tilde{\rho}) + \frac{1}{r}\ln\tilde{\rho} + \frac{\phi_1}{r_1}\ln\frac{\phi_1}{\omega_1} + \frac{\phi_2}{r_2}\ln\frac{\phi_2}{\omega_2}\right]\right\} \qquad (4)$$

where $\tilde{P}_i$, $\tilde{T}_i$, $\tilde{v}_i$, $\tilde{\rho}_i$ and $\tilde{P}$, $\tilde{T}$, $\tilde{v}$, $\tilde{\rho}$ are the reduced pressure, temperature, volume, and density of compo-

* To whom correspondence should be addressed.
[†] Chinese Academy of Sciences.
[‡] Jilin University.

10.1021/ma010023d CCC: $20.00
Published on Web 07/27/2001

nent i and the mixture, respectively, which are respectively defined as

$$\tilde{P}_i = P/P^*_i \quad \tilde{P} = P/P^* \tag{5}$$

$$\tilde{T}_i = T/T^*_i \quad \tilde{T} = T/T^* \tag{6}$$

$$\tilde{v}_i = V_i/V^*_i \quad \tilde{v} = V/V^* \tag{7}$$

$$\tilde{\rho}_i = 1/\tilde{v}_i \quad \tilde{\rho} = 1/\tilde{v} \tag{8}$$

Scaling parameters P^*_i, T^*_i, V^*_i and P^*, T^*, V^* can also be expressed in terms of the total interaction energy per mer and the close-packed volume per mer (the volume of a lattice site)

$$P^*_i = \epsilon^*_{ii}/v^*_i \quad P^* = \epsilon^*/v^* \tag{9}$$

$$T^*_i = \epsilon^*_{ii}/k \quad T^* = \epsilon^*/k \tag{10}$$

$$V^*_i = r^0_i N_i v^*_i \quad V^* = (r_1N_1 + r_2N_2)v^* = rNv^* \tag{11}$$

where ϵ^*_{ii}, v^*_i and ϵ^*, v^* are the total interaction energy per mer and the close-packed volume per mer of component i and the mixture, respectively; k represents the Boltzmann constant; r^0_i and r_i are the numbers of the lattice sites occupied by a molecule of component i in the pure fluid and the fluid mixture, respectively; r is the average number of the lattice sites occupied by a molecule in the fluid mixture; and N_i and N are the molecular numbers of component i and the mixture, respectively. Parameters ω^0_i and ω_i (in eqs 2 and 4) are the numbers of the configurations available to a r^0_i-mer and a r_i-mer in the close-packed states, respectively.

In the SL theory, the following energy-combining and volume-combining rules are used to calculate the total interaction energy per mer, ϵ^*, and the close-packed volume per mer, v^*, of a binary mixture, respectively

$$\epsilon^* = \phi_1{}^2\epsilon^*_{11} + 2\phi_1\phi_2\epsilon^*_{12} + \phi_2{}^2\epsilon^*_{22} \tag{12}$$

$$1/v^* = \phi_1/v^*_1 + \phi_2/v^*_2 \tag{13}$$

where ϕ_i stands for the close-packed volume fraction of component i in the mixture and ϵ^*_{12} is the interaction energy of a mer belonging to component 1 when it is surrounded by z mers belonging to component 2.

The Gibbs energy of mixing per mer, $\Delta\bar{\bar{G}}_M$, is defined as

$$\Delta\bar{\bar{G}}_M = \bar{\bar{G}}_M - (\phi_1\bar{\bar{G}}_1 + \phi_2\bar{\bar{G}}_2) \tag{14}$$

On the basis of the FH lattice model,[10] the FH interaction parameter, γ, can be expressed as

$$\gamma = \frac{\dfrac{\Delta G^{FH}_M}{kTV} - \left(\dfrac{\varphi_1}{V_1}\ln\varphi_1 + \dfrac{\varphi_2}{V_2}\ln\varphi_2\right)}{\varphi_1\varphi_2} \tag{15}$$

where V is the total volume of a binary polymer system; V_i and φ_i represent the molecular volume and the volume fraction of component i, respectively; and ΔG^{FH}_M is the Gibbs energy of mixing in the FH theory.

Table 1. Materials' Sources and Molecular Characteristics

polymer	supplier	M_w ($\times 10^4$)	M_n ($\times 10^4$)
PMMA	Acros	38.7	10.4
SAN	Aldrich	14.9	5.6

According to our previous assumptions,[35,36] eq 15 can be rewritten by means of the SL theory

$$\gamma = \frac{1}{(v^*\tilde{v})\phi_1\phi_2}\left\{\frac{-\tilde{\rho} + \tilde{P}\tilde{v}}{\tilde{T}} - \left[\phi_1\frac{-\tilde{\rho}_1 + \tilde{P}_1\tilde{v}_1}{\tilde{T}_1} + \phi_2\frac{-\tilde{\rho}_2 + \tilde{P}_2\tilde{v}_2}{\tilde{T}_2}\right] + (\tilde{v} - 1)\ln(1 - \tilde{\rho}) + \frac{1}{r}\ln\tilde{\rho} - \left[\phi_1\left((\tilde{v}_1 - 1)\ln(1 - \tilde{\rho}_1) + \frac{1}{r^0_1}\ln\tilde{\rho}_1\right) + \phi_2\left((\tilde{v}_2 - 1)\ln(1 - \tilde{\rho}_2) + \frac{1}{r^0_2}\ln\tilde{\rho}_2\right)\right] + \phi_1\left(\frac{1}{r^0_1}\ln\omega^0_1 - \frac{1}{r_1}\ln\omega_1\right) + \phi_2\left(\frac{1}{r^0_2}\ln\omega^0_2 - \frac{1}{r_2}\ln\omega_2\right)\right\} \tag{16}$$

Experimental Section

Materials. The sources and molecular characteristics of poly(methyl methacrylate) (PMMA) and poly(styrene-*co*-acrylonitrile) (SAN) with an acrylonitrile content of about 30 wt % used in this work are listed in Table 1. The materials were used as received without further purification. The weight and number-average molecular weights were determined by means of gel permeation chromatography relative to the polystyrene standards.

Sample Preparation. The PMMA powder and the SAN pellets were dried under vacuum at 80 °C for 24 h. The films of PMMA, SAN and their various blends were respectively prepared by casting from 5% (g/cm^3) 1,2-dichloroethane solutions. After the evaporation of the solvent (at room temperature), the films were further dried under vacuum at 80 °C for 3 days and finally at 120 °C for 2 days to ensure the complete removal of the solvent.

***PVT* Measurements.** The *PVT* properties of all the samples were determined with a commercial high-pressure piston-type dilatometer, a PVT-100 apparatus (SWO Polymertechnik GmbH), by means of an isothermal cooling procedure, in the temperature and pressure ranges 30−180 °C and 200−1800 bar, respectively, with 3 °C temperature and 200 bar pressure steps. The cooling rate was 1 °C min^{-1}. Every measured temperature was kept for 15 min and then increasing pressure measurements were performed. The data at 1 bar were extrapolated from those at high-pressure by means of the Tait equation of state.[37]

Results and Discussion

***PVT* Diagram.** The *PVT* properties of PMMA, SAN, and their blends, similar to those shown in Figure 1, were determined with a PVT-100 dilatometer. The experimental data were determined as a series of isotherms. Figure 1 presents the selected isobars with the interval of pressure 600 bar and the so-called isobar determined at 1 bar (open circles) is extrapolated one. Figure 1 shows the specific volume, V_{sp}, of PMMA as a function of temperature and pressure. The open squares represent the experimental data, and the solid lines AB and CD separate the diagram into three parts; with the increase of temperature, the three parts are glassy, exceptional, and melt states, respectively. In the exceptional area, a glass is reformed by pressurization from the melt during isothermal compression.[38] From Figure 1, it can be seen that the change of the specific volume

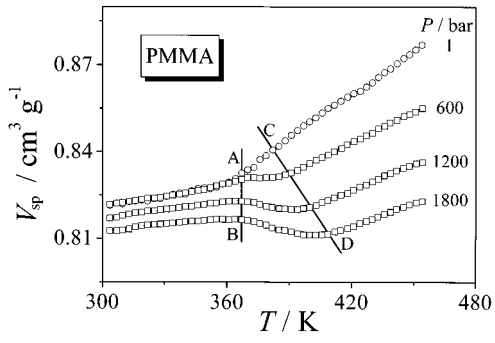

Figure 1. Specific volume, V_{sp}, of PMMA as a function of temperature and pressure. The open squares and circles represent the experimental data and the extrapolated 1 bar data, respectively, and the solid lines AB and CD separate the diagram into three parts: glassy, exceptional, and melt states.

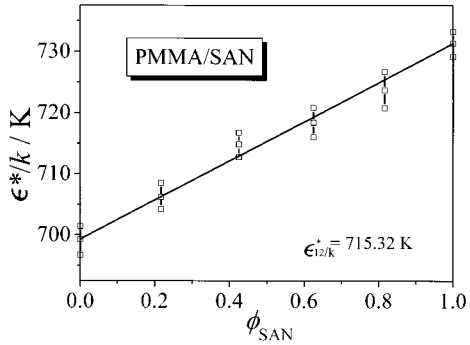

Figure 2. Interaction energy parameter, ϵ^*/k, as a function of the blend composition for the PMMA/SAN system. The open squares and the solid line represent the values evaluated with the SL equations of state and eq 12, respectively.

Table 2. Scaling Parameters of PMMA and SAN

polymer	P^* (bar)	ρ^* (kg m^{-3})	T^* (K)	$v^* \times 10^{29}$ (m^3 mer^{-1})
PMMA	6713.9	1300.7	699.3	1.4381
SAN	5886.8	1174.2	731.3	1.7152

in the glassy state is much smaller than that in the melt state with the changes of temperature and pressure. The specific volume decreases rapidly with the increase of pressure in the melt state. For all the samples, only the data of the equilibrium melt state were used to obtain the scaling parameters by fitting the *PVT* data to the SL equations of state as described above.

Scaling Parameters. Fitting the *PVT* data of the equilibrium melt state to the SL equations of state, i.e., eqs 1 and 3, we obtained three scaling parameters P^*, ρ^*, and T^* (or ϵ^*, v^*, and r) of all the samples. The scaling parameters of PMMA and SAN are listed in Table 2. In our previous paper,[35] the only one adjustable interaction energy parameter, ϵ^*_{12}/k, in the SL lattice fluid theory was evaluated by comparing the theoretical and the experimental phase diagrams. In this system, however, ϵ^*_{12}/k can be identified as 715.32 K by evaluating the scaling parameter, T^* (equals ϵ^*/k) of all the samples with the SL energy-combining rule (eq 12). Figure 2 shows ϵ^*/k as a function of the blend composition for the PMMA/SAN system. The open squares and the solid line represent the values evaluated with the SL equations of state and eq 12, respectively. During the evaluation of the scaling parameters for all the samples, the data of the equilibrium melt state within the same range (from 1 bar (117−174 °C), 200 bar (120−174 °C), and 400 bar (123−174 °C), to 1800 bar (144−174 °C)) were selected. From Figure 2, it can be seen that the SL energy-combining rule fits very well with the values evaluated from the *PVT* data. The adjustable interaction energy parameter, ϵ^*_{12}/k, supposed to be independent of temperature, was further used to calculate the spinodals, the binodals, the FH interaction parameter, the enthalpy of the mixing, and the combinatorial and vacancy entropies of the mixing.

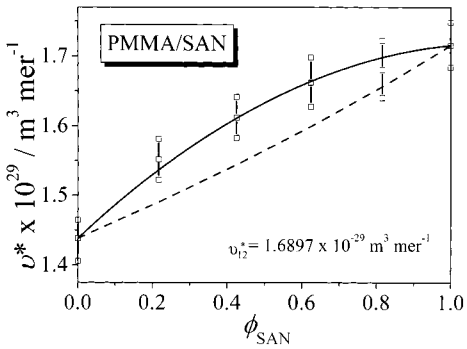

Figure 3. Close-packed volume per mer, v^*, as a function of the blend composition for the PMMA/SAN system. The open squares and the solid and dashed lines represent the values evaluated with the SL equations of state, eq 17, and calculated with eq 13, respectively.

The close-packed volume per mer, v^* (another scaling parameter), as a function of the blend composition for the PMMA/SAN system is shown in Figure 3. The open squares and the dashed line represent the values fitted with the SL equations of state and calculated with eq 13, respectively, which do not coincide well with each other. Therefore, we replace the SL volume-combining rule (eq 13) with the following equation which is similar to the combining rules presented by Panayiotou[39−41] in the SL lattice fluid theory and by Shiomi et al.[42] in a modified version of the FOV theory

$$v^* = \phi_1^2 v^*_1 + 2\phi_1\phi_2 v^*_{12} + \phi_2^2 v^*_2 \qquad (17)$$

where the adjustable volume mixing parameter, v^*_{12}, can be identified as 1.6897×10^{-29} m^3 mer^{-1} by fitting the values of the open squares to the new volume-combining rule (eq 17). From Figure 3, it can be seen that the open squares coincide very well with the solid line (evaluated with eq 17), that is, the new volume-combining rule is better than the original one for the PMMA/SAN system.

Spinodals and Binodals. Just as the spinodals and binodals of ternary and quaternary polymer blends were calculated with the method[43,44] (the knowledge of the first and second derivatives of ΔG with respect to the composition variables is not required), the spinodals and the binodals of the PMMA/SAN system were calculated with the SL theory by means of the two different volume-combining rules. Figure 4 shows the calculated results of the spinodals and the binodals compared with the experimental data obtained from references.[16,45] The dashed and the solid lines represent the spinodals and the binodals calculated with the SL theory by means of the new and the original volume-combining rules, respectively; the open and the solid squares represent the experimental spinodals and binodals, respectively, which were determined by Song et al.[45] for a PMMA/SAN system with an acrylonitrile content of 30 wt %, and the solid circles represent the experimental binodals determined by Suess et al.[16] for a PMMA/SAN system

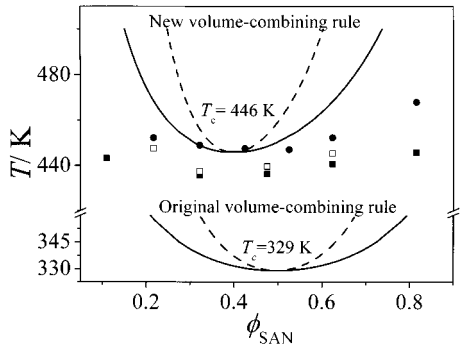

Figure 4. Spinodals and binodals of the PMMA/SAN system. The dashed and the solid lines represent the spinodals and the binodals calculated with the SL theory by means of the new (eq 17) and the original (eq 13) volume-combining rules, respectively; the open and the solid squares represent the experimental spinodals and binodals, respectively, which were determined by Song et al.,[45] and the solid circles represent the experimental binodals determined by Suess et al.[16]

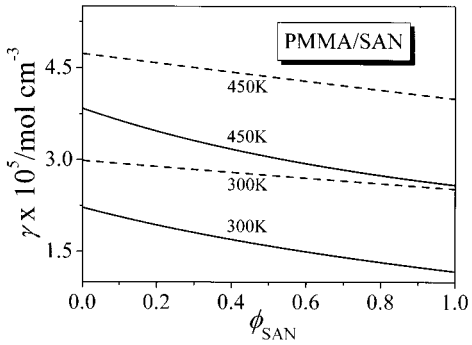

Figure 5. Temperature and blend composition dependences of the FH interaction parameter, γ, for the PMMA/SAN blends. The solid and the dashed lines represent the values calculated with eq 16 by means of the new (eq 17) and the original (eq 13) volume-combining rules, respectively.

with an acrylonitrile content of 30.5 wt %. From Figure 4, it can be seen that the critical temperature (T_c) calculated by means of the new volume-combining rule (446 K) is close to those determined by Song et al. (436 K) and by Suess et al. (447 K). However, the T_c calculated with the aid of the original volume-combining rule (329 K) is far from the experimental data. That is to say, the spinodals and the binodals calculated via the new volume-combining rule can be used to describe the phase diagrams for the PMMA/SAN system with LCST, whereas those calculated with the original one cannot. Moreover, according to our calculations, the phase diagram for the PMMA/SAN system is very sensitive to the adjustable volume mixing parameter, v^*_{12}.

FH Interaction Parameter. The FH interaction parameter, γ, was calculated with eq 16 by means of the two different volume-combining rules. Figure 5 shows the temperature and blend composition dependences of γ for the PMMA/SAN blends. The solid and the dashed lines represent the values calculated with eq 16 by using the new and the original volume-combining rules, respectively. From Figure 5, it can be seen that the two different volume-combining rules have a little influence on γ. The values of γ calculated with eq 16 by means of the new rule decrease with the increase of the SAN content in the blends under the isothermal conditions and are a little smaller than those calculated with eq 16 by means of the original rule under the same conditions. As shown in Figure 5, the lower the temperature, the smaller the values of the FH interaction parameter; that is to say, the miscibility of the PMMA/SAN blends can be improved by decreasing the temperature. Frezzotti et al.[46] gave the values of the interaction parameters, $\chi_{(1,2)}$, for a 50:50 (by weight) PMMA/SAN (containing 24 wt % acrylonitrile) blend, approaching -2.9×10^{-4} and -2.7×10^{-5} at 29.4 and 49.3 °C, respectively, and the corresponding values of the FH interaction parameter, γ, are calculated to be about -2.75×10^{-5} and -2.56×10^{-6} mol cm^{-3}, respectively, which are close to our calculated results.

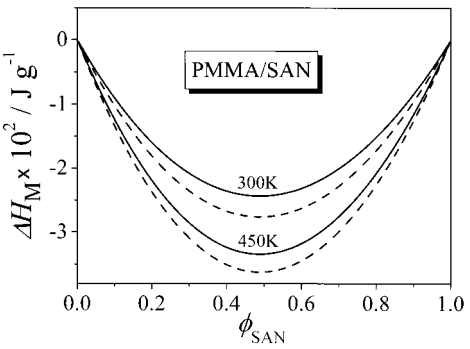

Figure 6. Temperature and blend composition dependences of the enthalpy of the mixing, ΔH_M, for the PMMA/SAN blends. The solid and the dashed lines represent the values calculated with eq 18 by means of the new (eq 17) and the original (eq 13) volume-combining rules, respectively.

Enthalpy of Mixing. It is known that the Gibbs energy can be split into its enthalpic and entropic parts in the SL theory.[13,14] The enthalpy of mixing per mer, $\Delta\bar{H}_M$, is given by

$$\Delta\bar{\bar{H}}_M = \frac{\Delta H_M}{rN} = \bar{\bar{H}}_M - \phi_1\bar{\bar{H}}_1 - \phi_2\bar{\bar{H}}_2 = \epsilon^*(-\tilde{\rho} + \tilde{P}\tilde{v}) - \phi_1\epsilon^*_{11}(-\tilde{\rho}_1 + \tilde{P}_1\tilde{v}_1) - \phi_2\epsilon^*_{22}(-\tilde{\rho}_2 + \tilde{P}_2\tilde{v}_2) \quad (18)$$

where $\bar{\bar{H}}_M$ and $\bar{\bar{H}}_i$ are the enthalpies per mer of the blend and component i, respectively. Figure 6 shows the temperature and blend composition dependences of ΔH_M for the PMMA/SAN blends. The solid and the dashed lines represent the values calculated with eq 18 by means of the new and the original volume-combining rules, respectively. From Figure 6, it can be seen that the values of ΔH_M calculated with eq 18 by means of the original volume-combining rule are a little more negative than those calculated with eq 18 by means of the new rule under the same conditions. Moreover, the higher the temperature, the more negative the enthalpy of the mixing. In the whole blend composition range, the enthalpy of the mixing is negative, which is favorable for the mixing of PMMA and SAN. It is generally recognized that an exothermic (negative) enthalpy of mixing between two polymers with a high molecular weight is a requirement for their miscibility.[15,47,48] Frezzotti et al.[46] determined the enthalpy of the mixing for forming a 50:50 (by weight) PMMA/SAN (containing 24 wt % acrylonitrile) blend by the Hess law on dilute polymer solutions and gave the values of ΔH_M, -1.94×10^{-3} and -2.00×10^{-4} J g^{-1}, approach at 29.4 and 49.3 °C, respectively. The absolute values of ΔH_M we calculated are approximately 1 order of magnitude higher than the experimental values obtained by Frezzotti et al. The reason for this difference appears to be the limited precision of the two methods. Moreover,

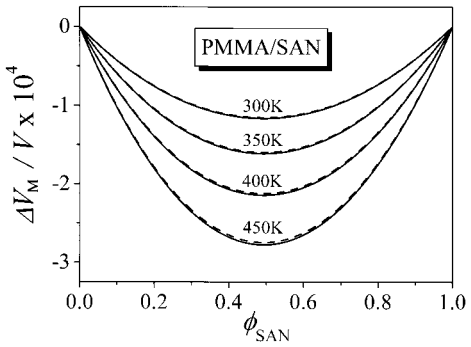

Figure 7. Temperature and blend composition dependences of the fractional volume change of the mixing, $\Delta V_M/V$, for the PMMA/SAN blends. The solid and the dashed lines represent the values calculated with eq 20 by means of the new (eq 17) and the original (eq 13) volume-combining rules, respectively.

according to our calculations, the enthalpy of the mixing for the PMMA/SAN blends is not sensitive to the adjustable volume mixing parameter, v^*_{12}.

Volume Change of Mixing. In the SL theory,[13,14] volume changes upon mixing are calculable. The volume change of mixing, ΔV_M, and the fractional volume change of mixing, $\Delta V_M/V$, are respectively given by

$$\Delta V_M = V - V_1 - V_2 = V^*\tilde{v} - V^*_1\tilde{v}_1 - V^*_2\tilde{v}_2 \quad (19)$$

$$\frac{\Delta V_M}{V} = 1 - \frac{1}{\tilde{v}}(\phi_1\tilde{v}_1 + \phi_2\tilde{v}_2) \quad (20)$$

where V_i and V are the volumes of component i (before blending) and the blend, respectively. Figure 7 shows the temperature and blend composition dependences of $\Delta V_M/V$ for the PMMA/SAN blends. The solid and the dashed lines represent the values calculated with eq 20 by means of the new and the original volume-combining rules, respectively. The calculated results suggest that the two different volume-combining rules do not nearly have influence on $\Delta V_M/V$. From Figure 7, it can be seen that the values of $\Delta V_M/V$ are negative, which favors the mixing of PMMA and SAN. Moreover, the higher the temperature, the more negative the values of $\Delta V_M/V$ are; that is, increasing temperature is favorable for the mixing of PMMA and SAN.

Combinatorial and Vacancy Entropies of Mixing. The entropic part of the Gibbs energy can be further split into the combinatorial and the lattice vacancy entropies.[49] The combinatorial entropy of mixing per mer, $\Delta\bar{\bar{S}}_{M,comb}$, and the vacancy entropy of mixing per mer, $\Delta S_{M,vac}$, can be respectively expressed as follows

$$\Delta\bar{\bar{S}}_{M,comb} = \frac{\Delta S_{M,comb}}{rN} = \bar{\bar{S}}_{M,comb} - \phi_1\bar{\bar{S}}_{1,comb} - \phi_2\bar{\bar{S}}_{2,comb} \quad (21)$$

$$\Delta\bar{\bar{S}}_{M,vac} = \frac{\Delta S_{M,vac}}{rN} = \bar{\bar{S}}_{M,vac} - \phi_1\bar{\bar{S}}_{1,vac} - \phi_2\bar{\bar{S}}_{2,vac} \quad (22)$$

where $\bar{\bar{S}}_{M,comb}$, $\bar{\bar{S}}_{i,comb}$ and $\bar{\bar{S}}_{M,vac}$, $\bar{\bar{S}}_{i,vac}$ are the combinatorial and the vacancy entropies per mer of the blend and component i, respectively. According to eqs 2, 4, and 14, the combinatorial and the vacancy entropies of mixing per mer contributing to the Gibbs energy of

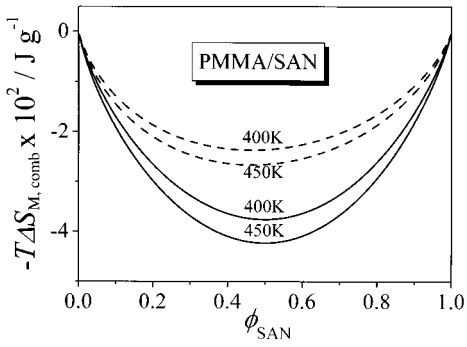

Figure 8. Temperature and blend composition dependences of $-T\Delta S_{M,comb}$ for the PMMA/SAN blends. The solid and the dashed lines represent the values calculated with eq 23 by means of the new (eq 17) and the original (eq 13) volume-combining rules, respectively.

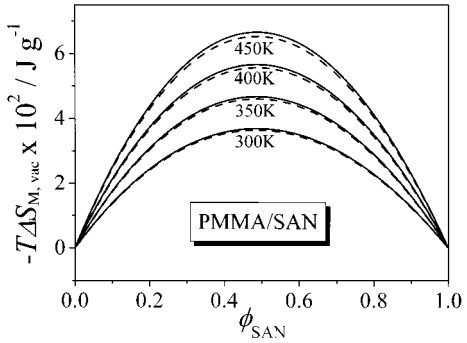

Figure 9. Temperature and blend composition dependences of $-T\Delta S_{M,vac}$ for the PMMA/SAN blends. The solid and the dashed lines represent the values calculated with eq 24 by means of the new (eq 17) and the original (eq 13) volume-combining rules, respectively.

mixing per mer can be respectively calculated by the following equations:

$$-T\Delta\bar{\bar{S}}_{M,comb} = \epsilon^*\tilde{T}\left(\frac{\phi_1}{r_1}\ln\frac{\phi_1}{\omega_1} + \frac{\phi_2}{r_2}\ln\frac{\phi_2}{\omega_2}\right) - \epsilon^*_{11}\tilde{T}_1\frac{\phi_1}{r_1^0}\ln\frac{1}{\omega_1^0} - \epsilon^*_{22}\tilde{T}_2\frac{\phi_2}{r_2^0}\ln\frac{1}{\omega_2^0} \quad (23)$$

$$-T\Delta\bar{\bar{S}}_{M,vac} = \epsilon^*\tilde{T}\left[(\tilde{v}-1)\ln(1-\tilde{\rho}) + \frac{1}{r}\ln\tilde{\rho}\right] - \phi_1\epsilon^*_{11}\tilde{T}_1\left[(\tilde{v}_1-1)\ln(1-\tilde{\rho}_1) + \frac{1}{r_1^0}\ln\tilde{\rho}_1\right] - \phi_2\epsilon^*_{22}\tilde{T}_2\left[(\tilde{v}_2-1)\ln(1-\tilde{\rho}_2) + \frac{1}{r_2^0}\ln\tilde{\rho}_2\right] \quad (24)$$

Figure 8 shows the temperature and blend composition dependences of $-T\Delta S_{M,comb}$ for the PMMA/SAN blends. The solid and the dashed lines represent the values calculated with eq 23 by means of the new and the original volume-combining rules, respectively. In Figure 8, there exhibits an influence of the two different volume-combining rules on $-T\Delta S_{M,comb}$. The temperature and blend composition dependences of $-T\Delta S_{M,vac}$ for the PMMA/SAN blends are shown in Figure 9. The solid and the dashed lines represent the values calculated with eq 24 by means of the new and the original volume-combining rules, respectively. The calculated results suggest that the two different volume-combining rules do not nearly have influence on $-T\Delta S_{M,vac}$.

From Figures 8 and 9, it can be seen that, in the whole blend composition range, $-T\Delta S_{M,comb}$ is negative, which is favorable for the decreasing of the Gibbs energy of mixing, whereas $-T\Delta S_{M,vac}$ is just opposite to $-T\Delta S_{M,comb}$. Moreover, the absolute value of $-T\Delta S_{M,comb}$ is smaller than that of $-T\Delta S_{M,vac}$ under the same conditions. Therefore, the total entropy of mixing contribution, $-T\Delta S_M$, is positive, which is unfavorable for the decreasing of the Gibbs energy of mixing. As shown in Figure 9, the higher the temperature, the more positive the value of $-T\Delta S_{M,vac}$. That is to say, the vacancy entropy of mixing is more unfavorable for the decreasing of the Gibbs energy of mixing with the increase of temperature. From the comparison of Figure 6 with Figure 9, we can see that the absolute value of ΔH_M is a little smaller than that of $-T\Delta S_{M,vac}$. Considered the contribution of the combinatorial entropy of the mixing, however, the Gibbs energy of mixing is negative, which is a necessary condition for the miscibility of PMMA and SAN.

Conclusions

According to the results obtained and the above discussion, some conclusions can be drawn, as follows.

(1) The new volume-combining rule presented in this paper can replace the original one, and the former coincides with the values (of v^*) evaluated with the SL equations of state better than the latter does. These two volume-combining rules have a slight influence on the FH interaction parameter, the enthalpy of mixing, and the combinatorial entropy of mixing.

(2) The spinodals and the binodals calculated with the SL theory by means of the new volume-combining rule can be used to describe the phase diagrams for the PMMA/SAN system with an LCST, whereas those calculated with the SL theory by means of the original one cannot.

(3) The FH interaction parameter indicates that the miscibility of the PMMA/SAN system can be improved by decreasing the temperature.

(4) In the whole blend composition range, the enthalpy of mixing and the volume change of mixing are negative, which is favorable for the mixing of PMMA and SAN.

(5) The combinatorial entropy of mixing is favorable for the decreasing of the Gibbs energy of mixing, whereas the vacancy entropy of mixing is just opposite to the former.

Acknowledgment. This work was supported by the Fund for Excellent Youth of China (No. 59825113), the National Natural Science Foundation of China (No. 20074037, 50073023), the Special National Natural Science Foundation of China (No. 20023003, 50027001), and the Special Funds for Major State Basic Research Projects (No. G1999064800). We also wish to acknowledge the Alexander von Humboldt-Stiftung for the support of the PVT-100 dilatometer.

References and Notes

(1) Freeman, P. I.; Rowlinson, J. S. *Polymer* **1960**, *1*, 20−26.
(2) Patterson, D. *Macromolecules* **1969**, *2*, 672−677.
(3) Biros, J.; Zeman, L.; Patterson, D. *Macromolecules* **1971**, *4*, 30−35.
(4) Bank, M.; Leffingwell, J.; Thies, C. *J. Polym. Sci., Part A-2* **1972**, *10*, 1097−1109.
(5) McMaster, L. P. *Macromolecules* **1973**, *6*, 760−773.
(6) Bernstein, R. E.; Cruz, C. A.; Paul, D. R.; Barlow, J. W. *Macromolecules* **1977**, *10*, 681−686.
(7) Kambour, R. P.; Bendler, J. T.; Bopp, R. C. *Macromolecules* **1983**, *16*, 753−757.
(8) Flory, P. J. *J. Chem. Phys.* **1942**, *10*, 51.
(9) Huggins, M. L. *Ann. N. Y. Acad. Sci.* **1942**, *43*, 1−32.
(10) Flory, P. J. *Principles of Polymer Chemistry*; Cornell University Press: Ithaca, NY, 1953; Chapter 12.
(11) Flory, P. J.; Orwoll, R. A.; Vrij, A. *J. Am. Chem. Soc.* **1964**, *86*, 3507−3514, 3515−3520.
(12) Sanchez, I. C.; Lacombe, R. H. *J. Phys. Chem.* **1976**, *80*, 2352−2362.
(13) Sanchez, I. C.; Lacombe, R. H. *Macromolecules* **1978**, *11*, 1145−1156.
(14) Lacombe, R. H.; Sanchez, I. C. *J. Phys. Chem.* **1976**, *80*, 2568−2580.
(15) Fower, M. E.; Barlow, J. W.; Paul, D. R. *Polymer* **1987**, *28*, 1177−1184, 2145−2150.
(16) Suess, M.; Kressler, J.; Kammer, H. W. *Polymer* **1987**, *28*, 957−960.
(17) Naito, K.; Johnson, G. E.; Allara, D. L.; Kei, T. K. *Macromolecules* **1978**, *11*, 1260−1265.
(18) Schäfer, R.; Zimmermann, J.; Kressler, J.; Mülhaupt, R. *Polymer* **1997**, *38*, 3745−3752.
(19) Mcbrierty, V. J.; Douglass, D. C.; Kwei, T. K. *Macromolecules* **1978**, *11*, 1265−1267.
(20) Feng, H.; Ye, C.; Feng, Z. *Polym. J.* **1996**, *28*, 661−664.
(21) Stein, V. D. J.; Jung, R. H.; Illers, K. H.; Hendus, H. *Angew. Makromol. Chem.* **1974**, *36*, 89−100.
(22) Kressler, J.; Higashida, N.; Inoue, T.; Heckmann, W.; Seitz, F. *Macromolecules* **1993**, *26*, 2090−2094.
(23) Ikawa, K.; Uemura, A.; Hosoda, S.; Kojima, T.; Nomura, H.; Chikaishi, K.; Amemiya, Y. *Polym. J.* **1991**, *23*, 1291−1296.
(24) Song, M.; Jiang, B. *Polymer* **1992**, *33*, 1445−1448.
(25) Jelenic, J.; Kirste, R. G.; Schmitt, B. J.; Schmitt-Strecker, S. *Makromol. Chem.* **1979**, *180*, 2057−2059.
(26) Hahn, K.; Schmitt, B. J.; Kirschey, M.; Kirste, R. G.; Salie, H.; Strecher, S. S. *Polymer* **1992**, *33*, 5150−5166.
(27) Kim, E.; Kramer, E. J.; Wu, W. C.; Garrett, P. D. *Polymer* **1994**, *35*, 5706−5715.
(28) Song, M.; Hammiche, A.; Pollock, H. M.; Hourston, D. J.; Reading, M. *Polymer* **1995**, *36*, 3313−3316.
(29) Hsu, W. P. *J. Appl. Polym. Sci.* **1999**, *74*, 2894−2899.
(30) Hong, Z.; Shaw, M. T.; Weiss, R. A. *Macromolecules* **1998**, *31*, 6211−6216.
(31) Madbouly, S. A.; Ougizawa, T.; Inoue, T. *Macromolecules* **1999**, *32*, 5631−5636.
(32) Li, W.; Radosz, M. *Polym. Prepr.* **1992**, *33*, 422−423.
(33) Shimomai, K.; Higashida, N.; Ougizawa, T.; Inoue, T.; Rudolf, B.; Kressler, J. *Polymer* **1996**, *37*, 5877−5882.
(34) Kim, Y. H.; Okamoto, M.; Kotaka, T. *Macromolecules* **2000**, *33*, 8113−8116.
(35) An, L.; Horst, R.; Wolf, B. A. *J. Chem. Phys.* **1997**, *107*, 2597−2602.
(36) Sun, Z.; An, L.; Jiang, Z.; Ma, R.; Wu, Z. *J. Macromol. Sci.—Phys.* **1999**, *B38*, 67−74.
(37) Tait, P. G. *Phys. Chem.* **1889**, *2*, 1.
(38) Schmidt, M.; Maurer, F. H. J. *J. Polym. Sci., B: Polym. Phys.* **1998**, *36*, 1061−1080.
(39) Panayiotou, C. *Macromolecules* **1987**, *20*, 861−871.
(40) Panayiotou, C. *Makromol. Chem. Soc.* **1986**, *187*, 2867−2882.
(41) Panayiotou, C. *Polym. Eng. Sci.* **1984**, *24*, 1219.
(42) Shiomi, T.; Hamada, F.; Nasako, T.; Yoneda, K.; Imai, K.; Nakajima, A. *Macromolecules* **1990**, *23*, 229−233.
(43) Horst, R. *Macromol. Theory Simul.* **1995**, *4*, 449−458.
(44) Horst, R.; Worf, B. A. *J. Chem. Phys.* **1995**, *103*, 3782−3787.
(45) Song, M.; Liang, H.; Jiang, B. *Chin. Polym. Acta* **1990**, *2*, 176−181.
(46) Frezzotti, D.; Ravanetti, G. P. *J. Therm. Anal.* **1994**, *41*, 1237−1243.
(47) Paul, D. R.; Barlow, J. W. *J. Macromol. Sci.—Rev. Macromol. Chem.* **1980**, *C18*, 109−168.
(48) Barlow, J. W.; Paul, D. R. *Annu. Rev. Mater. Sci.* **1981**, *11*, 299.
(49) Sanchez, I. C.; Balazs, A. C. *Macromolecules* **1989**, *22*, 2325−2331.

MA010023D